International Immunopharmacology 71 (2019) 224–232

Contents lists available at ScienceDirect

International Immunopharmacology

journal homepage: www.elsevier.com/locate/intimp

Selection and expression of CD40 single chain variable fragment by phage display and evaluation of tumor specific immune activation

Li Lu, Xi Wang, Ao Zhang, Fei Huang, Yongjia Yan, Weidong Li, Weihua Fu*

Department of General Surgery, Tianjin Medical University General Hospital, 154 Anshan Road, Heping District, Tianjin 300052, China

ARTICLE INFO

Keywords:
CD40
Phage display
ScFv
Tumor immunity

ABSTRACT

Immune escape is the final phase of the cancer immunoediting process. Researchers have found that cancer induces immune escape by inhibiting the expression of CD40L. The purpose of the present study was to select a high affinity CD40 single chain variable fragment (ScFv) and to evaluate its effect on tumor-specific immune activation. One Wistar rat was immunized with mouse CD40 antigen. CD40 ScFv with high affinity was constructed by overlap extension-polymerase chain reaction (SOE-PCR) and screened by three rounds of phage display. CD40 ScFv protein was expressed by the pET28a (+)-Rosetta prokaryotic expression system and purified using a nickel-nitrilotriacetic acid (Ni-NTA) column. CD40 ScFv significantly upregulated CD80, CD86, and MHC-II in vitro expression in dendritic cells (DCs) and upregulated the expression of IL-12 (p70) based on ELISA results. Cell counting kit-8 (CCK-8) results indicated that T lymphocytes were stimulated by DCs in an Ag + CD40 ScFv group, which also inhibited the proliferation of immortalized T6–17 cells. In an in vivo assay, 1×10^6 T6–17 cells were subcutaneously injected into BALB/c mice in the hind flank. Tumor volume curves showed that CD40 ScFv exhibited a remarkable inhibition of tumor proliferation after 15 days of treatment. Hematoxylin-eosin (H&E) staining of tumor tissues indicated that CD40 ScFv enhanced lymphocyte infiltration, which remarkably inhibited the proliferation of T6–17 cells. Furthermore, immunohistochemistry (IHC) staining revealed that caspase-3 was abundantly expressed in the T6–17 cytoplasm after CD40 ScFv treatment. In conclusion, this study revealed that high affinity CD40 ScFv could be screened by phage display and had a significant stimulating effect on DCs and inhibited the proliferation of T6–17 cells in vivo and in vitro.

1. Introduction

Immune escape is the final phase of the cancer immunoediting process, which prevents cancer cells from being destroyed by the immune system. Many cellular and molecular events govern cancer immune escape [1]. Based on these events, strategies have been designed to reverse tumor immune escape to develop promising therapeutic approaches for cancer patients [2].

CD40 is a cell surface glycoprotein belonging to the TNF receptor (TNFR) superfamily and plays a vital role in immune activation [3]. The CD40 ligand, CD40L is predominantly expressed on activated T lymphocytes and plays a crucial role in the maturation of dendritic cells (DCs) in combination with CD40 [4]. However, researchers have found that cancer could inhibit the expression of CD40L and inactivate the CD40-CD40L costimulatory pathway, which contributes toward cancer immune escape [5].

CD40 monoclonal antibodies such as CP-870,893 [6] and SGN-40 have been used in preclinical models and exhibited prominent antitumor effects. However, their associated side effects cannot be ignored, such as high liver metabolic burden and poor tissue penetration [6]. Single chain variable fragment (ScFv) is a particular form of antibody that combines variable heavy (VH) and variable light (VL) regions of a complete antibody by a flexible linker [7]. Although the molecular weight of ScFv (25–27 kDa) is lower than one-fifth of a complete antibody (150 kDa), the antigen binding ability of ScFv is the same as that of a complete antibody [8]. A number of ScFvs have been used for the treatment of cancer. Phage display is an efficient alternative to hybridoma technology for the production of therapeutically relevant antibodies [9]. Antibody phage display provides opportunities to design and construct large libraries of antibody fragments [10]. The expression of antibodies on the surface of phage particles represents a potent platform for the isolation of monoclonal antibodies (mAbs) with desired binding characteristics that can aid in the diagnoses and immunotherapies of different cancers. Phage display is an effective technique for the selection of tumor-specific recombinant human antibodies in vitro [11].

* Corresponding author at: Department of General Surgery, Tianjin Medical University General Hospital, 154 Anshan Road, Heping District, Tianjin 300052, China.
E-mail address: tjmughgs_fwh@163.com (W. Fu).

https://doi.org/10.1016/j.intimp.2019.03.020
Received 3 April 2018; Received in revised form 27 January 2019; Accepted 8 March 2019
Available online 26 March 2019

The present study utilized phage display technology to isolate potential positive ScFv clones from a phage library against mouse CD40 protein and characterization by phage enzyme-linked immune-sorbent assay (ELISA), DNA fingerprinting, and sequencing to obtain high affinity ScFv. Afterward, the immunostimulatory effects of the selected ScFv were assessed by flow cytometry and ELISA in vitro and hematoxylin-eosin (HE) and immunohistochemistry (IHC) staining in vivo.

2. Materials and methods

2.1. Animals and reagents

One female Wistar rat and several BALB/c (H2-d) mice (6–8 weeks old; 25–30 g weight) were purchased from the Animal Resource Center at the Institute of Radioactive Medicine, Chinese Academy of Medical Sciences (Tianjin, China). They were housed in a pathogen-free room with free access to autoclaved food and fresh water. All experimental protocols were reviewed and approved by the Institutional Animal Care and Use Committee of Tianjin Medical University. T6–17 cells, a genetically modified cell line derived from NIH/3T3 cells transfected with neu/c-erbB-2 oncogene, were granted as a gift from Professor Hongtao Zhang (University of Pennsylvania, Pennsylvania, USA). Rat anti-mouse CD40 mAb (FGK4.5) was purchased from BioXcell (West Lebanon, NH). pCANTAB5E phagemid (NEB, USA), FITC-CD80, PerCP-Cy5-5-CD86, and APC-MHC-II (BD Biosciences, USA) were used in the flow cytometry assay of DCs. Murine IL-12 (P70) and IFN-γ ELISA kits were all purchased from BOSTER Biosciences. Rabbit-anti-mouse caspase-3 antibody (Abcam, USA) and secondary goat-anti-rabbit IgG H&L antibody (Biotin; Abcam, USA) were used for the IHC detection of caspase-3 in tumor samples.

2.2. Construction of the phage display ScFv library

All genes encoding mouse VH and VL immunoglobulin sequences, including VH, kappa (Vκ), and lambda (Vλ) chains derived from B cells of Wistar rat immunized by mouse CD40 protein [12], were amplified by PCR for the phage library construction. Briefly, total RNA was prepared with TRIzol isolation reagent (Invitrogen, USA). cDNA was synthesized from RNA samples, and VH and VL genes were amplified with different primer mixtures by annealing to the constant regions of mouse VH and VL, respectively. VH and VL sequences were randomly linked via a $(Gly_4Ser)_3$ linker and cloned into pCANTAB5E phagemid with *Sfi*I restriction sites for VH and *Not*I for VL at the 5′ and 3′ ends, respectively. The presence and size of inserts were determined by sequencing of 13 separate colonies [13].

2.3. Bio-panning and isolation of CD40 ScFv

The bio-panning and isolation of CD40-specific ScFv were performed as described in the Human Single Fold ScFv Library (I + J) handbook with a few modifications. After the third-round panning, individual colonies were randomly selected and sequenced. Affinity to CD40 of the different clones was estimated by monoclonal phage-ELISA and gradient phage-ELISA as described by Salles et al. [14]. Murine CD40 protein (Sinobiological, China) was enveloped into a 96-well ELISA plate using CBS buffer. Then, 5 μg/mL and 100 μL/well were used in the monoclonal phage ELISA. In gradient phage ELISA, the concentrations of CD40 protein were 5 μg/mL, 2.5 μg/mL, 0.5 μg/mL, 0.1 μg/mL, and 0 μg/mL. The plate was incubated at 4 °C overnight after CD40 was embedded. Afterward, the ScFvs were subjected to affiliation, elution, and labeling by secondary antibody for microplate reader detection.

2.4. Expression and purification of CD40 ScFv

CD40 ScFv protein was expressed by *E. coli* Rosetta (DE3) (Invitrogen, USA) after transformation with recombinant pET28a (+)-CD40 ScFv. The expression of the soluble and insoluble protein fractions was examined by sodium dodecyl sulfate polyacrylamide gel electrophoresis (SDS-PAGE). Soluble ScFv was purified by a nickel-nitrilotriacetic acid (Ni-NTA) column (Kangweishiji Bio Inc., Beijing, China) and confirmed by western blot His-tag analysis. The endotoxin level of CD40 ScFv was evaluated semiquantitatively using a Tachypleus amebocyte lysate (TAL) kit (Zeyebiological, China) according to the manufacturer's protocols.

2.5. Assessment of CD40 ScFv-stimulated tumor-specific immunoreaction

Primary marrow stromal cells (MSCs) were isolated from mice femur. Bone marrow dendritic cells (BMDCs) were induced in complete DMEM supplemented with 10% fetal calf serum (FCS), granulocyte macrophage colony-stimulating factor (GM-CSF; 20 ng/mL) (PeproTech, USA) and interleukin-4 (IL-4; 10 ng/mL) (PeproTech, USA) at 37 °C in a 5% CO_2 humidified atmosphere. After 4 days of culture, T6–17 frozen-thawed antigen (Ag) (25 μg/mL) was added to the supernatant. After another 2 days of culture, CD40 ScFv (1 μg/mL), TNF-α (100 U/mL) (PeproTech, USA) and normal saline (NS) were added to the supernatant followed by another 2 days of incubation.

After 10 days of incubation, DCs were recovered by centrifugation at 1500 rpm (250*g*) for 5 min. Cell culture supernatant was recovered and stored in a sterile EP tube at 4 °C. The expression levels of CD80, CD86 and MHC-II on DCs were estimated by flow cytometry. IL-12 expression in the supernatant of DCs in different treatment groups was detected by ELISA according to the manufacturer's instructions.

Magnetic column (Miltenyi Biotec USA) purification was used to purify splenic $CD3^+$ T lymphocytes that had been incubated together with DCs of different treatment groups as previously described (the cell number ratio was DCs:T cells = 1:10). The proliferation of T lymphocytes in different treatment groups was detected by the CCK-8 test (DOJINDO, Japan). T cells in different treatment groups were recovered by centrifugation at 1500 rpm (250*g*) for 5 min. Cell culture supernatant was recovered and stored in a sterile EP tube at 4 °C. IFN-γ expression was estimated by ELISA according to the manufacturer's instructions. T6–17 cells were cultured and incubated together with T lymphocytes in different treatment groups. The CCK-8 test was implemented to evaluate the inhibition rate of T6–17 cells. The cell growth inhibition rate was calculated according to the formula: inhibition rate = (OD of control cells − OD of treated cells) / OD of control cells × 100%.

Then, 1×10^6 T6–17 cells in 100 μL of PBS were subcutaneously injected into the hind flank of BALB/c mice. After tumor models were confirmed, mice were randomly split into 3 groups ($n = 5$ for the CD40 ScFv group, CD40 mAb group and normal saline group). Mice received different implements by intratumoral injection: CD40 ScFv (750 μg/kg), CD40mAb (5 mg/kg) or NS. Treatments started from the first day when tumor establishment was confirmed (Day 0) and continued on Days 3, 6, 9, 12, 15, 18, and 21. Tumor volumes were calculated in cm^3 as $0.5 \times (\text{length})^3 \times (\text{width})^2$ after each treatment. After 8 treatments, mice were sacrificed at Day 24. Tumors were harvested and processed for histological staining, and caspase-3 expression was assessed by IHC as described in Qiu's study [15]. IHC staining and scoring were determined by two clinical pathologists, according to the proportion of positively stained cells and staining intensity. Five high power fields were randomly selected. Positively stained cells were scored as follows: 1 (< 10%), 2 (10–30%), 3 (30–60%), and 4 (> 60%). The staining intensity was graded as follows: 1 (light yellow), 2 (yellow to brown), 3 (brown), and 4 (deep brown). The staining index was determined by positive staining cells × staining intensity. Hematoxylin–eosin-stained slides were evaluated for stromal tumor infiltrating lymphocytes (TILs) using full sections in 10% increments (< 10%, 10% ~100%) by a pathologist blinded to the intervention of the mouse model, as recommended [16]. Four nonoverlapping fields with high numbers of TILs on the H&E-stained slides were selected.

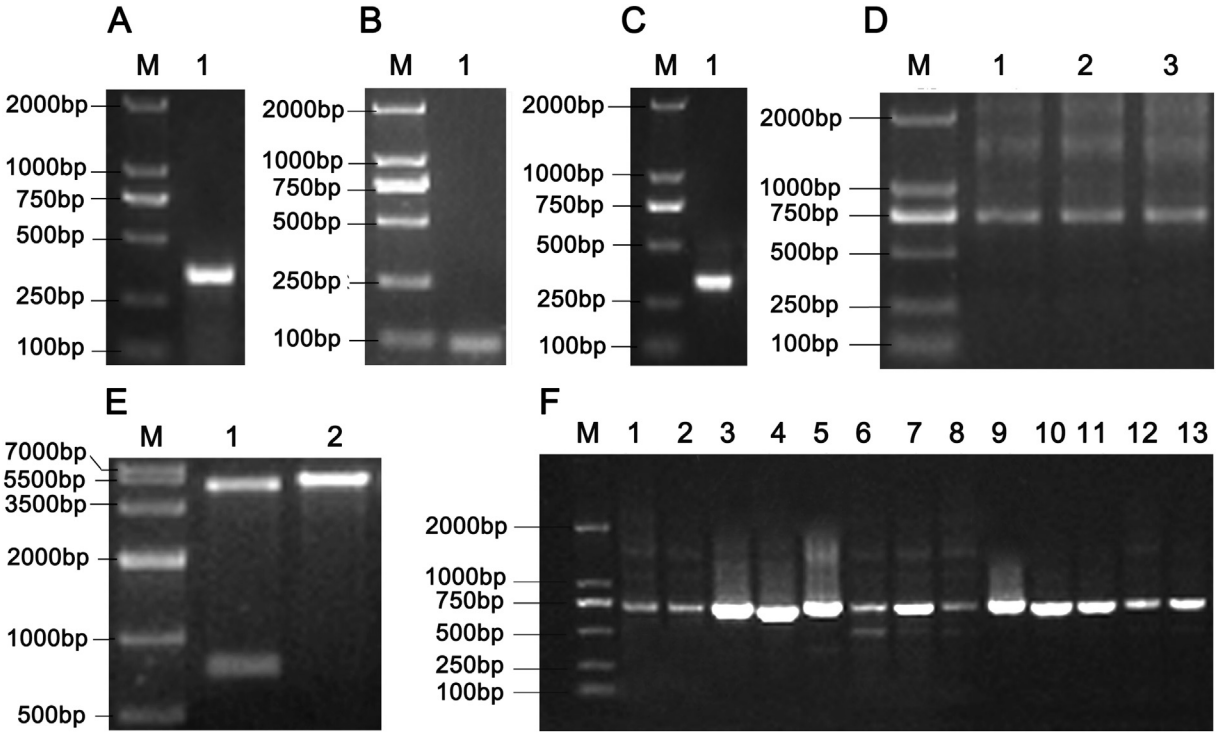

Fig. 1. Agarose gel electrophoresis of PCR.
A. 1. VH Fragment M: Marker DM2000; B. Linker; C. 1. VL Fragment M: Marker DM2000 D. 1, 2, 3: ScFv M: Marker DM2000; E. 1, 2: restriction analysis of pCANTAB5E-ScFv M: Marker IV; F. 1–13: random colony PCR of phage library M: Marker DM2000. CD40 ScFv contained 714 bp, which included 345 bp of V_H, 45 bp of Linker and 324 bp of V_L. The agarose gel electrophoresis results were consistent with the expected length. Two bands could be found in the double enzyme assay results, which were consistent with the length of pCANTAB5E (4522 bp) and ScFv (714 bp).

2.6. Statistical analysis

The results are presented as the mean ± SD of at least three separate experiments. The data were analyzed by one-way ANOVA for the comparison of variables among groups based on the homogeneity test of the data. The Student-Newman-Keuls multiple comparison test was used to compare two groups using PRISM software (GraphPad Software, Inc., San Diego, CA, USA). Significant differences were defined as $P < 0.05$.

3. Results

3.1. Construction of the anti-CD40 immunization phage display library

As shown in Fig. 1A, B, and C, VH, Linker and VL genes were amplified. In another strategy, VH and VL were amplified and linked through overlap PCR (Fig. 1D). Subsequently, the ScFv genes were cloned into the pCANTAB5E vector by enzymatic digestion (Fig. 1E). The library capacity was 1.2×10^7, and each of the ScFv genes had a real size insertion by random colony PCR (Fig. 1F).

3.2. Bio-panning of the high affinity CD40 ScFv clone by phage display

Three rounds of panning were carried out for the enrichment of anti-CD40 phage ScFv from the phage display library. Increasing numbers of output phages in each round indicated the validity of the panning (Fig. 2A). Polyclonal phage-ELISA demonstrated that after three rounds of panning, the OD450 value of Round 3 (3.02 ± 0.18) increased significantly ($F = 95.547$, $P = 0.000$) when compared with before panning (0.76 ± 0.103). This indicated that the affinity of the clones significantly increased (Fig. 2B).

After the third round of panning, 20 clones were randomly selected for monoclonal phage ELISA. Multi-alignments of sequences showed that 6 clones were excluded because the sequences were repetitive. Among the 14 clones, 8 clones reacted positively to CD40 with high OD values and low cross-reactivity with BSA (ratio > 4, Fig. 3A). Gradient phage ELISA demonstrated that following the decline of embedded CD40 concentration from 5 μg/mL to 0.1 μg/mL, clone $8^{\#}$ exhibited the highest affinity to CD40 antigen, which had significant differences when compared with the other clones (Fig. 3B). Therefore, clone $8^{\#}$ was affirmed as a positive clone for CD40 (CD40 ScFv).

3.3. Identification of CD40 ScFv by DNA sequencing and structure imitating

DNA sequencing indicated that clone $8^{\#}$ contained 714 bp, which included 345 bp of VH, 45 bp of Linker and 324 bp of VL. IMGT tests showed the VH and VL fragments had high matching scores with RadnorIGHV5-29*01 F and Ratnor IGKV10S12*01 F, respectively, which indicated the structural correctness of clone $8^{\#}$. Molecular models of CD40 ScFv were generated by *Protean* software: 115 amino acids in the VH (red color), 15 amino acids in the linker (green color), and 109 amino acids in the VL (blue color) (Fig. 4). The protein tertiary structure of CD40 ScFv was imitated by I-TASSER (https://zhanglab.ccmb.med.umich.edu/I-TASSER/output/S364859/). The C-score of the model was 0.93, and the estimated TM-score was 0.84 ± 0.08.

3.4. Expression and purification of CD40 ScFv

pET28a (+)-$8^{\#}$ was transformed into *E. coli* Rosetta (DE3) for the expression of soluble ScFv. SDS-PAGE demonstrated that 1 mM isopropyl-β-D-thiogalactoside (IPTG) more effectively induced CD40 ScFv protein expression (Fig. 5A). Protein was purified by Ni-NTA, and 200 mM imidazole exhibited the best eluting effect (Fig. 5C). To evaluate the expression of soluble ScFv protein, western blot assay was applied using anti-His-tag antibody. Representative results demonstrated a specific reactivity of anti-His-tag antibody with ScFv protein at

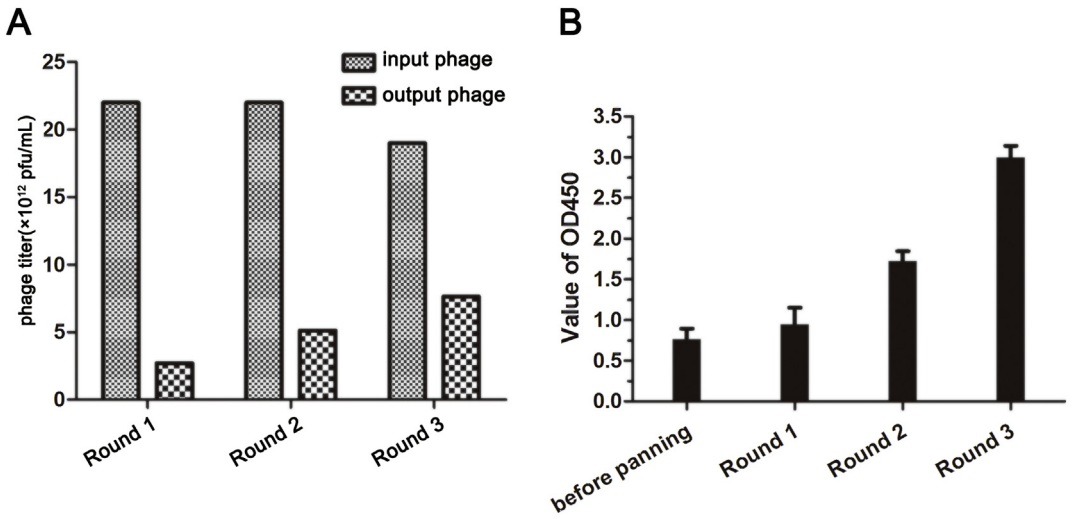

Fig. 2. Evaluation of the enrichment of the phage display library.
A. Titer of input phage and output phage in each round; B. evaluation of each round's library affinity progress by polyclonal phage-ELISA (n = 3). The increasing number of output phages in each round indicated the validity of panning. Polyclonal phage-ELISA also demonstrated that the affinity of the clones increased significantly.

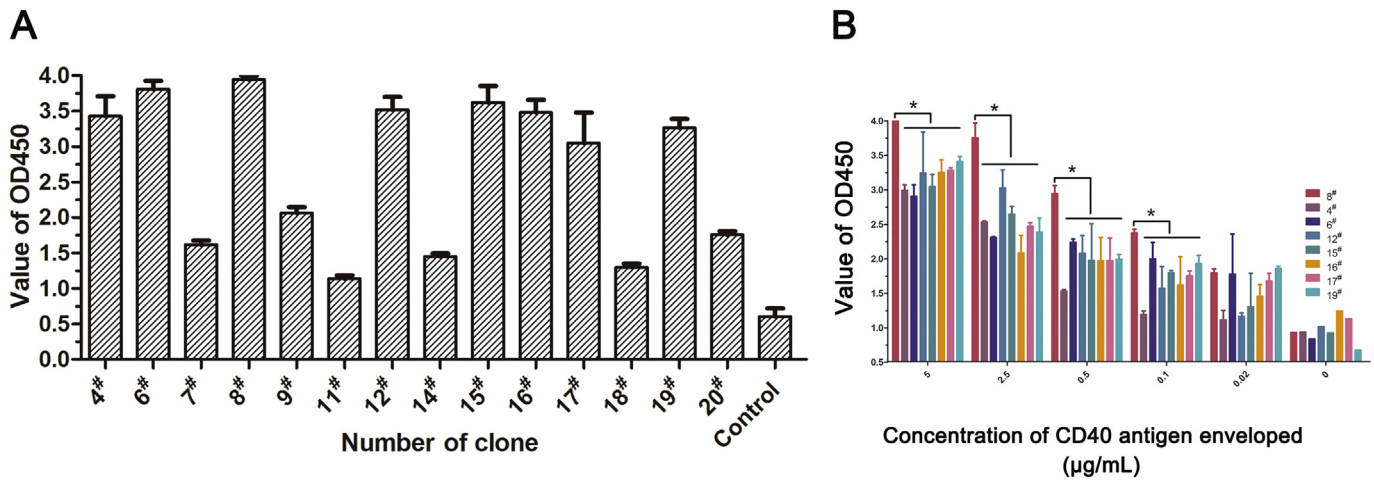

Fig. 3. Affinity assessment of different clones by phage ELISA.
A. Monoclonal phage ELISA of the random clones after the 3rd round of panning (n = 3). B. Gradient phage ELISA of potential positive clones (n = 3). Among the 14 different clones, 8 clones reacted positively to CD40 with high OD450 values and low cross-reactivity with BSA, ratio > 4. Gradient phage ELISA demonstrated that following the decline of embedded CD40 concentration from 5 μg/mL to 0.1 μg/mL, clone $8^{\#}$ exhibited the highest affinity to CD40 antigen (n = 3, *: $P < 0.05$).

the expected site (25 kDa). The concentration of CD40 ScFv was 1.122 mg/mL (Fig. 5B). The endotoxin level of prepared protein was assayed using a TAL kit and found to be lower than 0.79 EU/mL.

3.5. CD40 ScFv activated BMDCs resulting in improved T-cell responses

Mouse BMDCs stimulated by CD40 ScFv exhibited significantly upregulated expression of CD80, CD86 and MHC-II (Figs. 6A, B, C and S1), similar to previous observations with CD40 agonists [17]. A notable increase in IL-12p70 secretion was detected after CD40 ScFv stimulation (Fig. 6D); a similar pattern ($P > 0.05$) was observed in the Ag + TNF-α group. IFN-γ ELISA indicated that T cells could be stimulated by mature BMDCs after interference by CD40 ScFv (Fig. 6E).

3.6. CD40 ScFv inhibited the proliferation of T6–17 and generated tumor-specific immune responses

We evaluated whether the CD40 ScFv could enhance tumor-specific immune responses. T6–17 cells were cultured and incubated with T lymphocytes in different treatment groups. The CCK-8 test was applied to evaluate the inhibition rate of T6–17 cells. After frozen-thawed antigens of T6–17 tumor cells (Ag) were phagocytized and generated in T lymphocytes, CD40 ScFv caused a dramatic inhibition of T6–17 cells by stimulating tumor-specific T lymphocytes. The inhibition rate was higher than those of the NS and Ag groups ($P < 0.05$), which is dominantly attributed to the maturation of BMDCs and stimulation of tumor-specific CTL (Fig. 7).

After co-culture with matured DCs, T lymphocytes were activated by antigen presentation and co-stimulating signal. This induced the apoptosis of tumor cells by a cytotoxic effect. CCK-8 tests indicated that CD40 ScFv caused a dramatic inhibition of T6–17 cells by stimulating tumor-specific T lymphocytes.

CD40 ScFv induced T6–17 cell apoptosis by activating T lymphocytes in vivo.

T6–17 tumor models in mice were constructed (Fig. S2). After treatment, mice were sacrificed. The differences in tumor volumes at each time point of the three groups were evaluated, and the results showed no significant differences between the three groups from Day 0

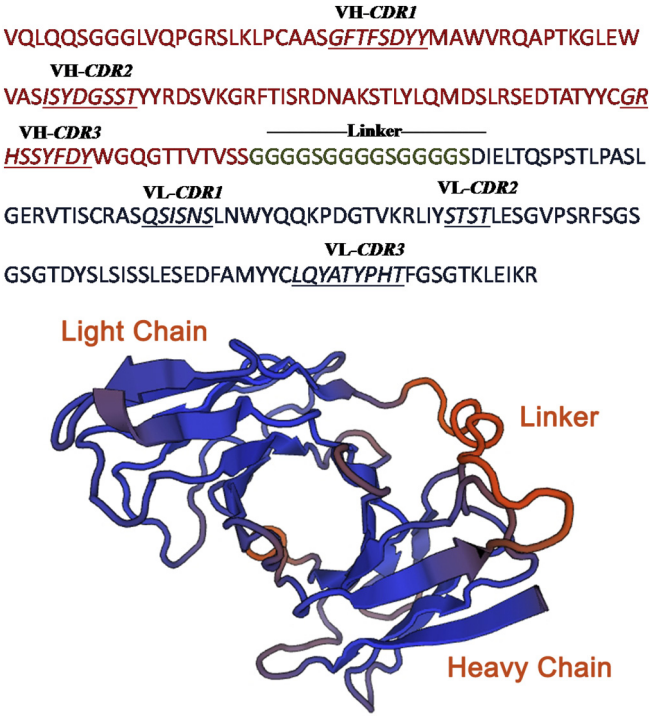

Fig. 4. Structural analysis of CD40 ScFv.
Relying on the IMGT analysis, the CDR region of VH and VL could be identified and labeled. Based on the amino acid sequence, the tertiary structure of CD40 ScFv was predicted by I-TASSER.

to Day 12. Until Day 15, CD40 ScFv and CD40 mAb exhibited remarkable inhibition of tumor proliferation when compared with the NS group (Table 1). The TIL ratios in the different treatment groups were evaluated based on the HE staining of tumor tissues. The results indicated that, when compared with the NS group, CD40 ScFv and CD40 mAb significantly enhanced lymphocyte infiltration in tumor tissue ($F = 55.30$, $P = 0.000$) and markedly inhibited the proliferation of T6–17 cells. No significant differences were observed between the CD40 ScFv group (70.0 ± 14.0)% and the CD40 mAb group (72.5 ± 5.00)% ($P = 0.708$). The expression of caspase-3 in different treatment groups was scored as previously described. The results indicated that caspase-3 was abundantly expressed in the T6–17 cytoplasm after CD40 ScFv or CD40 mAb treatment ($F = 16.829$, $P = 0.000$). Significant differences were observed between the CD40 ScFv group (11.0 ± 3.082) and the NS group (2.80 ± 1.304) ($P = 0.000$). No significant differences were observed between the CD40 ScFv group and the CD40 mAb group (11.4 ± 3.130) ($P = 0.815$) (Fig. 8).

4. Discussion

CD40/CD40L is a costimulatory molecule. CD40 is mainly expressed on antigen presenting cells such as B lymphocytes and DCs. CD40L is mainly expressed in T lymphocytes, which can combine with CD40 and promote DC maturation. Therefore, the activation of a costimulatory pathway plays a decisive effect in the maturation of DCs, which contributes toward immune activation. However, in tumor microenvironments, cancer cells can inhibit the expression of CD40L by releasing immunosuppressive factors, thereby inhibiting DC maturation and the inactivation of cytotoxic T lymphocytes (CTLs), which are considered the most important mechanisms of cancer immune escape [18]. In recent years, CD40 agonists have been used in cancer therapy to induce the apoptosis of cancer cells by promoting DC maturation and stimulating T lymphocyte proliferation [19,20]. Treatment with anti-CD40 monoclonal antibodies has been exploited in several cancer immunotherapy studies in mice. This has led to the development of anti-CD40 antibodies for clinical use. As examples, Dacetuzumab [21] and Lucatumumab [22–26] have both exhibited promising treatment outcomes with low toxicity.

Humanized mAbs against tumor antigens have been considered for targeted therapies in cancer treatment. However, most humanized mAbs have been derived from mice, which have limited immunogenicity. As one of the most common recombinant antibodies, ScFv exhibits promising prospects in cancer treatment. Compared with monoclonal antibodies, ScFv has better tissue penetration ability and lower metabolic burden due to its lower molecular weight (25–27 kDa). In this study, CD40 ScFv was selected to elucidate the mechanism of tumor immunity activation by CD40 small-molecule agonist antibody and to provide a theoretical basis for future research. Based on the results of this study, we will continue to screen human CD40 ScFv to construct a CD40 × HER2 single chain diabody for potential applications in cancer treatment.

Phage display technology provides an alternative to traditional antibody production methods. This technique involves the selection of a number of high affinity antigen-reactive antibody fragments by employing recombinant phage libraries, which expose functional antigen binding sites on their surface. Phage display technology is widely used to isolate human ScFvs to recognize diverse proteins [27]. Based on different library constructions, phage display libraries can be divided into natural libraries and immunological libraries [28]. Natural antibody libraries are derived from animals or human B lymphocytes with good diversity and large library capacity [29]. However, the

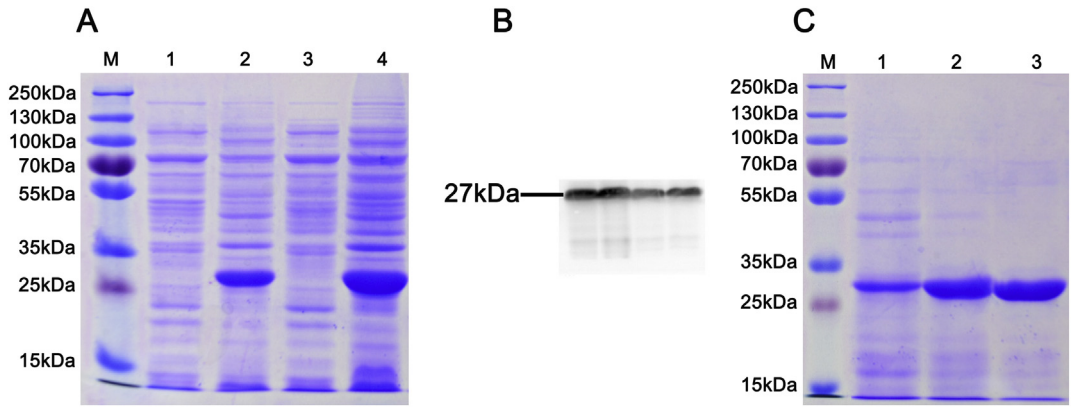

Fig. 5. Evaluation of the expression and purification of CD40 ScFv.
A. M Protein ladder; 1. bacterium spallation supernatant of 0.5 mM IPTG, 2. inclusion body of 0.5 mM IPTG, 3. bacterium spallation supernatant of 1 mM IPTG, 4. inclusion body of 1 mM IPTG; B. positive protein bands emerge around 25 kDa in the His-tag western blot; C. 1, eluent of 50 mM imidazole; 2, eluent of 100 mM imidazole; 3, eluent of 200 mM imidazole.

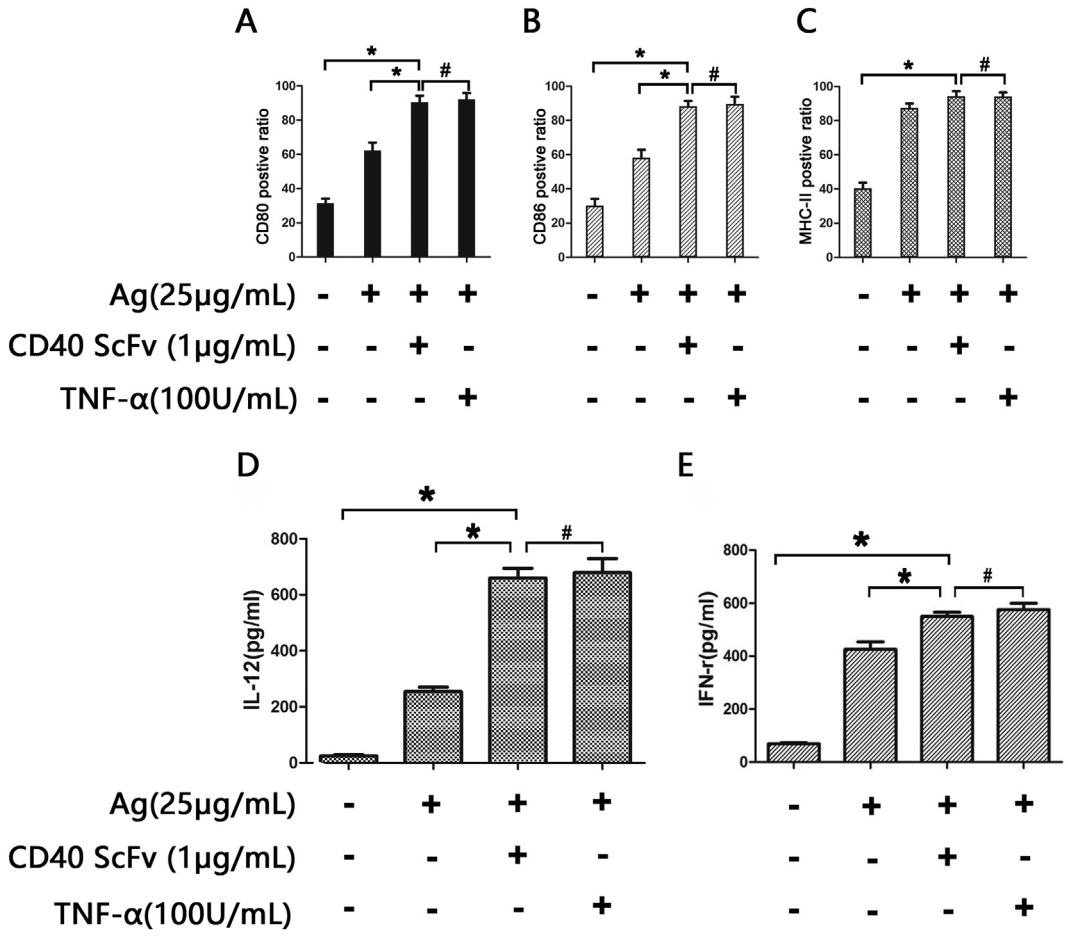

Fig. 6. CD40 ScFv activates BMDCs, resulting in improved T cell responses.
A. CD80 expression of different treatment groups (n = 3), B. CD86 expression of different treatment groups (n = 3), C. MHC-II expression of different treatment groups (n = 3), D. IL-12 expression of different treatment groups (n = 3), E. IFN-γ expression of different treatment groups (n = 3). After stimulation by CD40 ScFv, DCs exhibited significantly upregulated expression of CD80, CD86 and MHC-II, and a notable increase in IL-12p70 secretion was detected in the meantime. After co-culture with T lymphocytes, IFN-γ expression was markedly improved (*: $P < 0.05$, #: $P \geq 0.05$).

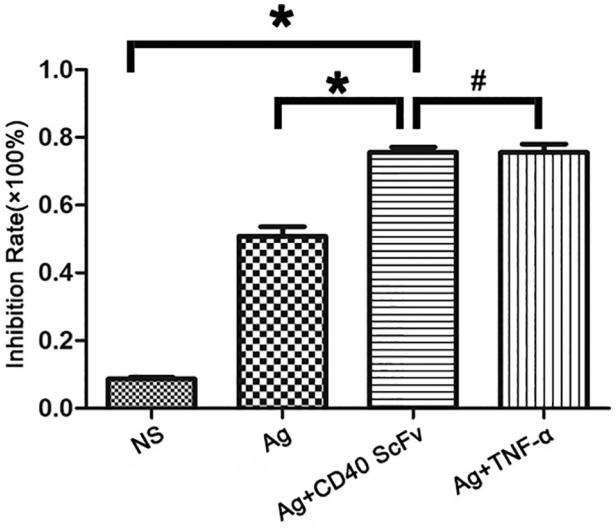

Fig. 7. Comparison of tumor inhibition rates of T6–17 cells in different treatment groups (*: $P < 0.05$, #: $P \geq 0.05$, n = 3).

construction process is complex and cannot be concentrated for any one specific antigen. Immunological libraries are constructed using specific antigens immunized to animals. Despite the relatively small capacities of these libraries, they have specific values for antigen immunization. Antigen-specific antibodies are predominantly distributed in these libraries [30]. Due to their convenient construction process and higher screening efficiency, an anti-CD40 immunization library was constructed for our research. The capacity of this library was 1.2×10^7 pfu/mL, and the sequencing results indicated good diversity. To select the best affinity clone after screening, phage ELISA and Gradient phage ELISA are typically employed. The criteria are often different and rely on different experiment design and screening programs. Aghebati [31] randomly selected clones after a final screening round and performed a phage ELISA. A positive clone was considered if the ratio of A490 values between the clone and a negative control group was > 3. Zhou [32] performed EGFRvIII antibody screening; the A490 value of the clone to be tested was defined as being > 2 times higher than the negative control group. In the present study, based on our lower filter, we defined potential clones as those having an A490 value ratio of at least 4.

CD80 and CD86 belong to a costimulatory adhesion molecule family that activates T cells through a costimulatory pathway. They have been used as indicators of DC maturation in most studies. MHC-II, as the principal component of antigen presentation, is significantly elevated after antigen loading. Therefore, CD80, CD86 and MHC-II molecules have been considered markers of DC maturation [33]. IL-12 is also considered one of the more important parameters of DC maturation [34]. In our study, CD40 ScFv significantly upregulated CD80/CD86/MHC-II expression compared with the NS and Ag groups. IL-12

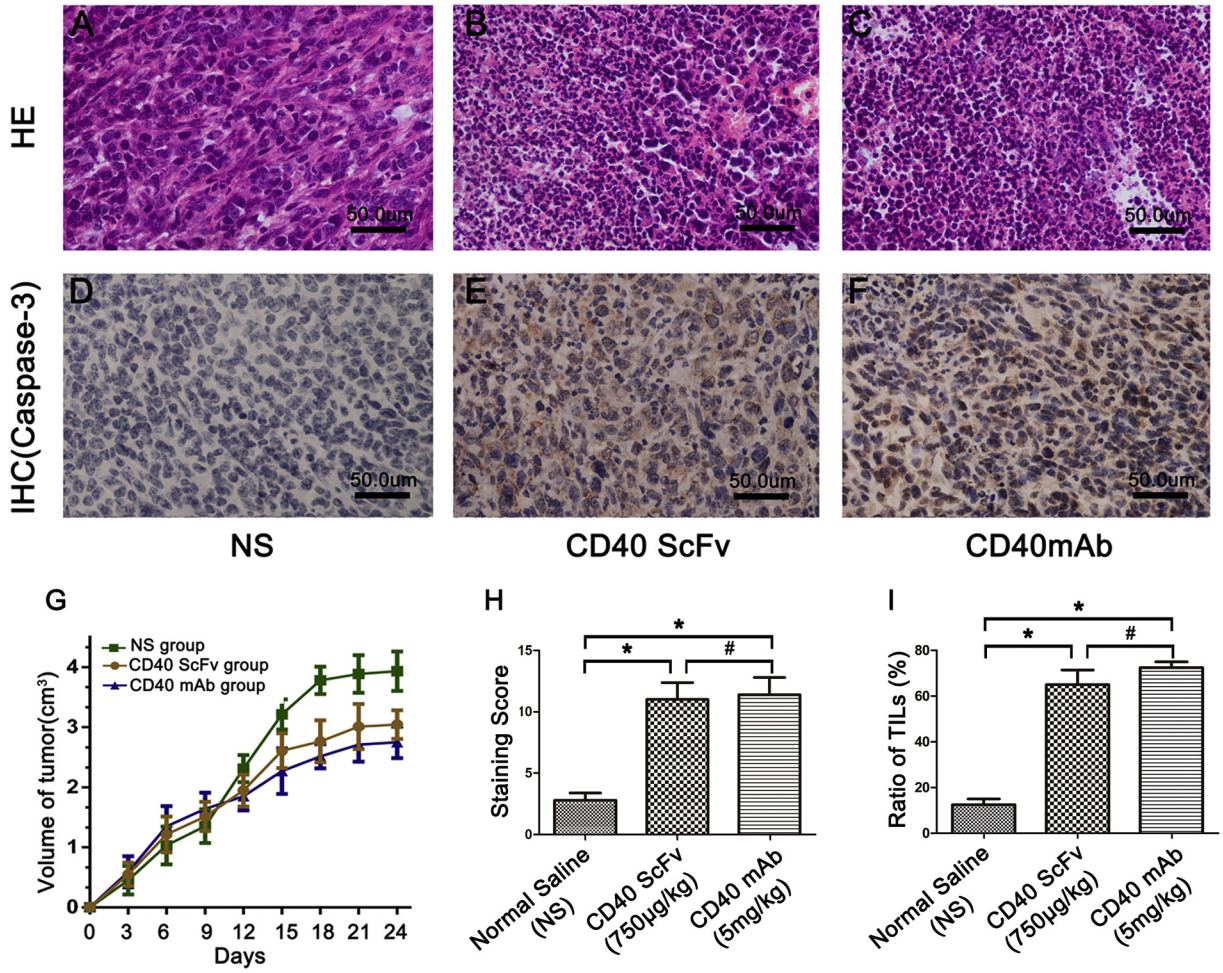

Fig. 8. CD40 ScFv inhibited the proliferation of T6–17 cells in BALB/c mice.
A–F. Cell morphology and caspase-3 expression in different treatment groups (n = 5 for the CD40 ScFv group, CD40 mAb group and normal saline group). Mouse tumor models were constructed successfully. The differences in tumor volume were evaluated, and the results demonstrated that until Day 15, CD40 ScFv exhibited a marked inhibition of tumor proliferation. HE staining indicated significant lymphocyte infiltration, and a notably increased expression of caspase-3 could be detected by IHC. G. T6–17 tumor growth curve in the BALB/c mouse model of different treatment groups. H. IHC staining score of caspase-3 in different treatment groups. I. Comparison of the TIL ratio in different treatment groups (n = 5, *: $P < 0.05$, #: $P \geq 0.05$).

Table 1
Comparison of tumor volumes at each time point in the three groups.

Day	Tumor volume (cm^3)			F	P
	CD40ScFv	NS	CD40mAb		
3	0.550 ± 0.196#	0.453 ± 0.237#	0.591 ± 0.259	0.483	0.760
6	1.214 ± 0.298#	1.032 ± 0.314#	1.350 ± 0.335	1.269	0.316
9	1.514 ± 0.242#	1.353 ± 0.282#	1.641 ± 0.270	1.481	0.264
12	1.945 ± 0.264#	2.310 ± 0.226#	1.850 ± 0.235	4.552	0.086
15	2.610 ± 0.290*#	3.214 ± 0.250	2.270 ± 0.381*	11.815	0.001
18	2.765 ± 0.349*#	3.780 ± 0.229	2.516 ± 0.201*	20.199	0.000
21	3.010 ± 0.375*#	3.886 ± 0.312	2.712 ± 0.286*	17.433	0.000
24	3.044 ± 0.239*#	3.933 ± 0.326	2.749 ± 0.261*	24.642	0.000

* Significant difference in comparison with the NS group ($P < 0.05$).
# No significant difference in comparison with the CD40mAb group ($P \geq 0.05$).

expression in the Ag + CD40 ScFv group was significantly increased compared with the NS and Ag groups. However, no significant differences between the Ag + CD40 ScFv and Ag + TNF-α groups were observed ($P > 0.05$). Our results were consistent with those of Mangsbo et al. [35]. Narayanan [36], after stimulating CD40 signaling pathways in DCs, observed significant upregulation of the expression of CD80/CD86/MHC-II, consistent with our results.

CTL plays a critical role in the antitumor immune response [37]. CTL can induce cancer cell apoptosis by secreting perforin and granzyme after stimulation by mature DCs. A previous study reported that CD40L-expressing DCs could deliver CD40–CD40L signaling to CD8 + T cells to induce CTL responses [38]. Therefore, we further evaluated the immune activation of CD40 ScFv by detecting the inhibition rate of T6–17 by CTL. Our results revealed that T lymphocytes activated by Ag + CD40 ScFv inhibited the proliferation of T6–17 cells with significant differences compared with the NS and Ag groups but not with the Ag + TNF-α group. A number of studies have shown that CD40mAb can inhibit tumor proliferation by activating tumor-specific immune responses in vivo [39]. Therefore, we used it as a positive control to evaluate the immune activation function of CD40 ScFv in vivo. The concentration of CD40 mAb was 5 mg/kg, which is the same concentration used in most studies [40,41]. Differences in tumor volumes were evaluated. The results demonstrated that until Day 15, CD40 ScFv exhibited a remarkable inhibition of tumor proliferation. Ruth [42], after 5 treatments with CD40 mAb and on the 8th day of treatment, showed a significantly decreased tumor size, which was similar to our results. We speculated that the immune activation of tumor cells is a systematic process involving multiple cell types.

Eriksson et al. [43] found that the activation of CD40-CD40L by CD40L gene therapy enhanced T-cell expansion and migration in the

tumor microenvironment. Therefore, we assessed tumor lymphocyte infiltration. Hematoxylin–eosin-stained slides for paired match cases were evaluated for stromal tumor infiltrating lymphocytes (TILs) based on previously described criteria. The results demonstrated that CD40 ScFv significantly enhanced lymphocyte infiltration when compared with the NS group. The main mechanism of CTL inhibition of tumor cells is to internalize granzymes [44], which ultimately induces apoptosis of tumor cells by activating Caspase-3. Caspase-3 is a critical protease in early stage apoptosis activation and is the final apoptotic executioner [45]. In many studies [46,47], Caspase-3 was used as an indicator for CTL function evaluation. In this study, IHC staining showed that Caspase-3 was abundantly expressed in the T6–17 cytoplasm after treatment with CD40 ScFv or CD40 mAb, which indicated that CD40 ScFv induced apoptosis of T6–17 cells by stimulating CTL.

In conclusion, we screened a high-affinity CD40 ScFv by phage display in a CD40 immunization library. CD40 ScFv stimulated DCs and inhibited the proliferation of T6–17 cells in vitro and in vivo.

Supplementary data to this article can be found online at https://doi.org/10.1016/j.intimp.2019.03.020.

Acknowledgments

This work was supported by the Tianjin Application Foundation and Frontier Technology Research Plan (15JCYBJC25200), the Tianjin Health Industry Key Projects (15KG148). In this study, Li Lu and Weihua Fu conceived and designed the experiments; Li Lu and Xi Wang performed the construction of the phage display ScFv library and screening of CD40 ScFv; Ao Zhang and Fei Huang performed the induction of DC in vitro and the construction of the tumor model; Yongjia Yan and Weidong Li performed IHC staining and tumor volume measurement; and Weihua Fu provided expertise in the whole experiment process.

References

[1] A. Chawla, G. Alatrash, Y. Wu, E.A. Mittendorf, Immune aspects of the breast tumor microenvironment, Breast Cancer Manag. 2 (3) (2013) 231–244, https://doi.org/10.2217/bmt.13.15.
[2] O. Hamid, C. Robert, A. Daud, F.S. Hodi, W.J. Hwu, R. Kefford, et al., Safety and tumor responses with lambrolizumab (anti-PD-1) in melanoma, N. Engl. J. Med. 369 (2013) 134–144, https://doi.org/10.1056/NEJMoa1305133.
[3] U. Schonbeck, P. Libby, The CD40/CD154 receptor/ligand dyad, Cell. Mol. Life Sci. 58 (2001) 4–43.
[4] Y. Kawashita, N.J. Deb, M.K. Garg, R. Kabarriti, Z. Fan, A.A. Alfieri, J. Roy-Chowdhury, C. Guha, Tumor-specific immunity and cure after radio-inducible suicide gene therapy and systemic CD40-ligand and Flt3-ligand gene therapy in an orthotopic tumor model, Radiat. Res. 182 (2) (2014) 201–210, https://doi.org/10.1667/RR13617.1.
[5] Y. Ma, G.V. Shurin, Z. Peiyuan, M.R. Shurin, Dendritic cells in the cancer microenvironment, J. Cancer 4 (1) (2013) 36–44, https://doi.org/10.7150/jca.5046.
[6] M. Heo, S. Kim, S. Kim, Y. Kim, J. Chung, M. Oh, S. Lee, Functional expression of single-chain variable fragment antibody against c-Met in the cytoplasm of Escherichia coli, Protein Expr. Purif. 47 (1) (2006) 203–209 47:203–209 https://doi.org/10.1016/j.pep.2005.12.003.
[7] Z.A. Ahmad, S.K. Yeap, A.M. Ali, W.Y. Ho, N.B.M. Alitheen, M. Hamid, scFv antibody: principles and clinical application, Clin. Dev. Immunol. 2012 (2012) 980250, , https://doi.org/10.1155/2012/980250.
[8] P. Holliger, P.J. Hudson, Engineered antibody fragments and the rise of single domains, Nat. Biotechnol. 23 (9) (2005) 1126–1136, https://doi.org/10.1038/nbt1142.
[9] P. Carter, Improving the efficacy of antibody-based cancer 437 therapies, Nat. Rev. Cancer 1 (2) (2001) 118–129, https://doi.org/10.1038/35101072.
[10] L. Aghebati-Maleki, B. Bakhshinejad, B. Baradaran, Phage display as a promising approach for vaccine development, J. Biomed. Sci. 23 (1) (2016) 66, https://doi.org/10.1186/s12929-016-0285-9.
[11] C.M. Hammers, J.R. Stanley, Antibody phage display: technique and applications, J. Invest. Dermatol. 134 (2) (2014) 1–5, https://doi.org/10.1038/jid.2013.521.
[12] Makvandinejad S, Sheedy C, Veldhuis L, et al. Selection of single chain variable fragment (scFv) antibodies from a hyperimmunized phage display library for the detection of the antibiotic monensin. J. Immunol. Methods, 2010, 360(2):103–118. DOI: https://doi.org/10.1016/j.jim.2010.06.015.
[13] M. Li, M. Zhu, C. Zhang, X. Liu, Y. Wan, Uniform orientation of biotinylated nanobody as an affinity binder for detection of bacillus thuringiensis (Bt) Cry1Ac toxin, Toxins 6 (2014) 3208–3222, https://doi.org/10.3390/toxins6123208.
[14] Salles B C, Costa L E, Alves P T, et al. Leishmania infantum mimotopes and a phage-ELISA assay as tools for a sensitive and specific serodiagnosis of human visceral leishmaniasis. Diagn. Microbiol. Infect. Dis., 2017;87(3):219–225. DOI: https://doi.org/10.1016/j.diagmicrobio.2016.11.012.
[15] X. Qiu, C. Klausen, J.C. Cheng, et al., CD40 ligand induces RIP1-dependent, necroptosis-like cell death in low-grade serous but not serous borderline ovarian tumor cells, Cell Death Dis. 6 (8) (2015) e1864, https://doi.org/10.1038/cddis.2015.229.
[16] R. Salgado, C. Denkert, S. Demaria, N. Sirtaine, F. Klauschen, G. Pruneri, S. Wienert, G. Van den Eynden, F.L. Baehner, F. Penault-Llorca, et al., The evaluation of tumor-infiltrating lymphocytes (TILs) in breast cancer: recommendations by an International TILs Working Group 2014, Ann. Oncol. 26 (2015) 259–271, https://doi.org/10.1093/annonc/mdu450.
[17] R.P. Gladue, T. Paradis, S.H. Cole, C. Donovan, R. Nelson, R. Alpert, J. Gardner, E. Natoli, E. Elliott, R. Shepard, V. Bedian, The CD40 agonist antibody CP-870,893 enhances dendritic cell and B-cell activity and promotes anti-tumor efficacy in SCID-hu mice, Cancer Immunol. Immunother. 60 (7) (2011) 1009–1017, https://doi.org/10.1007/s00262-011-1014-6.
[18] Y. Ma, G.V. Shurin, Z. Peiyuan, M.R. Shurin, Dendritic cells in the cancermicroenvironment, J. Cancer 4 (1) (2013) 36–44, https://doi.org/10.7150/jca.5046.
[19] A. Kosaka, T. Ohkuri, H. Okada, Combination of an agonistic anti-CD40 monoclonal antibody and the COX-2 inhibitor celecoxib induces anti-glioma effects by promotion of type-1 immunity in myeloid cells and T-cells, Cancer Immunol. Immunother. 63 (8) (2014) 847–857, https://doi.org/10.1007/s00262-014-1561-8.
[20] A. Khong, M.D. Brown, J.B. Vivian, B.W. Robinson, A.J. Currie, Agonistic anti-CD40 antibody therapy is effective against postoperative cancer recurrence and metastasis in a murine tumor model, J. Immunother. 36 (7) (2013) 365–372, https://doi.org/10.1097/CJI.0b013e31829fb856.
[21] R.R. Furman, A. Forero-Torres, A. Shustov, J.G. Drachman, A phase I study of dacetuzumab (SGN-40, a humanized anti-CD40 monoclonal antibody) in patients with chronic lymphocytic leukemia, Leuk. Lymphoma 51 (2) (2010) 228–235, https://doi.org/10.3109/10428190903440946.
[22] R. Kedar, O. Sabag, M. Licthenstein, H. Lorberboum-Galski, Soluble CD40 ligand (sCD40L) provides a new delivery system for targeted treatment: sCD40L-caspase 3 chimeric protein for treating B-cell malignancies, Cancer 118 (24) (2012) 6089–6104, https://doi.org/10.1002/cncr.27654.
[23] J.C. Byrd, T.J. Kipps, I.W. Flinn, M. Cooper, O. Odenike, J. Bendiske, J. Rediske, S. Bilic, J. Dey, J. Baeck, S. O'Brien, Phase I study of the anti-CD40 humanized monoclonal antibody lucatumumab (HCD122) in relapsed chronic lymphocytic leukemia, Leuk. Lymphoma 53 (11) (2012) 2136–2142, https://doi.org/10.3109/10428194.2012.681655.
[24] Y.T. Tai, X. Li, X. Tong, D. Santos, T. Otsuki, L. Catley, O. Tournilhac, K. Podar, T. Hideshima, R. Schlossman, P. Richardson, N.C. Munshi, M. Luqman, K.C. Anderson, Human anti-CD40 antagonist antibody triggers significant antitumor activity against human multiple myeloma, Cancer Res. 65 (13) (2005) 5898–5906, https://doi.org/10.1158/0008-5472.CAN-04-4125.
[25] R. Advani, A. Forero-Torres, R.R. Furman, J.D. Rosenblatt, A. Younes, H. Ren, K. Harrop, N. Whiting, J.G. Drachman, Phase I study of the humanized anti-CD40 monoclonal antibody dacetuzumab in refractory or recurrent non-Hodgkin's lymphoma, J. Clin. Oncol. 27 (26) (2009) 4371–4377, https://doi.org/10.1200/JCO.2008.21.3017.
[26] W. Bensinger, R.T. Maziarz, S. Jagannath, A. Spencer, S. Durrant, P.S. Becker, B. Ewald, S. Bilic, J. Rediske, J. Baeck, E.A. Stadtmauer, A phase 1 study of lucatumumab, a fully human anti-CD40 antagonist monoclonal antibody administered intravenously to patients with relapsed or refractory multiple myeloma, Br. J. Haematol. 159 (1) (2012) 58–66, https://doi.org/10.1111/j.1365-2141.2012.09251.x.
[27] Rahbarnia L, Farajnia S, Babaei H, et al. Evolution of phage display technology: from discovery to application. J. Drug Target., 2017, 25(3):216–224. DOI: https://doi.org/10.1080/1061186X.2016.1258570.
[28] M. Hamzeh-Mivehroud, A.A. Alizadeh, M.B. Morris, et al., Phage display as a technology delivering on the promise of peptide drug discovery, Drug Discov. Today 18 (23–24) (2013) 1144–1157, https://doi.org/10.1016/j.drudis.2013.09.001.
[29] P. Mondon, O. Dubreuil, K. Bouayadi, et al., Human antibody libraries: a race to engineer and explore a larger diversity, Front. Biosci. 13 (13) (2008) 1117–1129.
[30] P. Pansri, N. Jaruseranee, K. Rangnoi, P. Kristensen, M. Yamabhai, A compact phage display human ScFv library for selection of antibodies to a wide variety of antigens, BMC Biotechnol. 9 (2009) 6, https://doi.org/10.1186/1472-6750-9-6.
[31] L. Aghebati-Maleki, V. Younesi, F. Jadidi-Niaragh, et al., Isolation and characterization of anti ROR1 single chain fragment variable antibodies using phage display technique, Hum. Antibodies 25 (1–2) (2017) 57, https://doi.org/10.3233/HAB-170310.
[32] Min Zhou, Bi-zhi Shi, Jian-ren Gu, Zong-hai Li, Construction and screening of phage antibody libraries against epidermal growth factor receptor variant type III, China Biotechnol. (4) (2010) 1–7.
[33] Hunter T B, Alsarraj M, Gladue R P, et al. An agonist antibody specific for CD40 induces dendritic cell maturation and promotes autologous anti-tumour T-cell responses in an in vitro, mixed autologous tumour cell/lymph node cell model. Scand. J. Immunol., 2007, 65(5):479–486. DOI: https://doi.org/10.1111/j.1365-3083.2007.01927.x.
[34] V. Athie-Morales, H.H. Smits, D.A. Cantrell, C.M. Hilkens, Sustained IL-12 signaling is required for Th1 development, J. Immunol. 172 (1) (2004) 61–69.
[35] Mangsbo S M, Broos S, Fletcher E, et al. The human agonistic CD40 antibody ADC-1013 eradicates bladder tumors and generates T-cell-dependent tumor immunity. Clin. Cancer Res., 2014, 21(5):1115–26. DOI: https://doi.org/10.1158/1078-0432.CCR-14-0913.

[36] P. Narayanan, A composite MyD88/CD40 switch synergistically activates mouse and human dendritic cells for enhanced antitumor efficacy, J. Clin. Investig. 121 (4) (2011) 1524–1534, https://doi.org/10.1172/JCI44327.
[37] R.M. Zinkernagel, P.C. Doherty, Immunological surveillance against altered self -components by sensitised T lymphocytes in lymphocytic choriomeningitis, Nature 251 (5475) (1974) 547–548.
[38] Johnson S1, Y. Zhan, R.M. Sutherland, A.M. Mount, S. Bedoui, J.L. Brady, E.M. Carrington, L.E. Brown, G.T. Belz, W.R. Heath, et al., Selected Toll-like receptor ligands and viruses promote helper-independent cytotoxic T cell priming by upregulating CD40L on dendritic cells, Immunity 30 (2) (2009) 218–227, https://doi.org/10.1016/j.immuni.2008.11.015.
[39] A. Khong, A.L. Cleaver, M. Fahmi Alatas, B.C. Wylie, T. Connor, S.A. Fisher, S. Broomfield, W.J. Lesterhuis, A.J. Currie, R.A. Lake, et al., The efficacy of tumor debulking surgery is improved by adjuvant immunotherapy using imiquimod and anti-CD40, BMC Cancer 14 (1) (2014) 969, https://doi.org/10.1186/1471-2407-14-969.
[40] Zhang M1, W. Ju, Z. Yao, P. Yu, B.R. Wei, R.M. Simpson, R. Waitz, M. Fassò, J.P. Allison, T.A. Waldmann, Augmented interleukin (IL)-15Rα expression by CD40 activation is critical in synergistic CD8 T-cell mediated antitumor activity of anti-CD40 antibody with IL-15 in TRAMP-C2 tumors in mice, J. Immunol. 188 (12) (2012) 6156, https://doi.org/10.4049/jimmunol.1102604.
[41] J. Medina-Echeverz, C. Ma, A.G. Duffy, T. Eggert, N. Hawk, D.E. Kleiner, F. Korangy, T.F. Greten, Systemic agonistic anti-CD40 treatment of tumor bearing mice modulates hepatic myeloid suppressive cells and causes immune-mediated liver damage, Cancer Immunol. Res. 3 (5) (2015), https://doi.org/10.1158/2326-6066.CIR-14-0182.
[42] R.R. French, H.T. Chan, A.L. Tutt, M.J. Glennie, CD40 antibody evokes a cytotoxic T-cell response that eradicates lymphoma and bypasses T-cell help, Nat. Med. 5 (5) (1999) 548–553, https://doi.org/10.1038/8426.
[43] Eriksson E, Moreno R, Milenova I, Liljenfeldt L, Dieterich LC, Christiansson L, Karlsson H, Ullenhag G, Mangsbo SM, Dimberg A, et al. Activation of myeloid and endothelial cells by CD40L gene therapy supports T-cell expansion and migration into the tumor microenvironment. Gene Ther., 2017, 24(2):92–103. DOI: https://doi.org/10.1038/gt.2016.80.
[44] J. Li, S.K. Figueira, A.C. Vrazo, et al., Real-time detection of CTL function reveals distinct patterns of caspase activation mediated by Fas versus granzyme B, J. Immunol. 193 (2) (2014) 519, https://doi.org/10.4049/jimmunol.1301668.
[45] X. Liu, H. Zou, C. Slaughter, et al., DFF, a heterodimeric protein that functions downstream of caspase-3 to trigger DNA fragmentation during apoptosis, Cell 89 (2) (1997) 175–184, https://doi.org/10.4049/jimmunol.1301668.
[46] L. He, J. Hakimi, D. Salha, et al., A sensitive flow cytometry-based cytotoxic T-lymphocyte assay through detection of cleaved caspase 3 in target cells, J. Immunol. Methods 304 (1–2) (2005) 43–59, https://doi.org/10.4049/jimmunol.1301668.
[47] K.R. Jerome, D.D. Sloan, M. Aubert, Measurement of CTL-induced cytotoxicity: the caspase 3 assay, Apoptosis 8 (6) (2003) 563.